LEBANESE AMERICAN UNIVERSITY

Effect of blood viscosity on the atherosclerotic plaque: A Fluid-Structure Interaction Model

By

Yara H. Zgheib

A thesis

Submitted in partial fulfillment of the

requirements

for the degree of Master of Science in

Applied and Computational Mathematics

School of Arts and Science

June 2022

LAU
الجامعة اللبنانية الأميركية
Lebanese American University

THESIS APPROVAL FORM

Student Name: Yara Zgheib I.D. #: 202004685

Thesis Title: Effect of blood viscosity on the atherosclerotic plaque: A Fluid-Structure Interaction Model

Program: Master of Applied and Computational Mathematics

Department: Computer Science and Mathematics

School: Arts and Sciences

The undersigned certify that they have examined the final electronic copy of this thesis and approved it in Partial Fulfillment of the requirements for the degree of:

Master in Applied and Computational Mathematics

Thesis Advisor's Name: Nader El Khatib

Signature: [redacted] Date: 20 / 06 / 2022 (Day / Month / Year)

Committee Member's Name: Chadi Nour

Signature: [redacted] Date: 20 / 06 / 2022 (Day / Month / Year)

Committee Member's Name: Jean Takchi

Signature: [redacted] Date: 20 / 06 / 2022 (Day / Month / Year)

LAU
الجامعة اللبنانية الأميركية
Lebanese American University

THESIS COPYRIGHT RELEASE FORM

LEBANESE AMERICAN UNIVERSITY NON-EXCLUSIVE DISTRIBUTION LICENSE

By signing and submitting this license, you (the author(s) or copyright owner) grants the Lebanese American University (LAU) the non-exclusive right to reproduce, translate (as defined below), and/or distribute your submission (including the abstract) worldwide in print and electronic formats and in any medium, including but not limited to audio or video. You agree that LAU may, without changing the content, translate the submission to any medium or format for the purpose of preservation. You also agree that LAU may keep more than one copy of this submission for purposes of security, backup and preservation. You represent that the submission is your original work, and that you have the right to grant the rights contained in this license. You also represent that your submission does not, to the best of your knowledge, infringe upon anyone's copyright. If the submission contains material for which you do not hold copyright, you represent that you have obtained the unrestricted permission of the copyright owner to grant LAU the rights required by this license, and that such third-party owned material is clearly identified and acknowledged within the text or content of the submission. IF THE SUBMISSION IS BASED UPON WORK THAT HAS BEEN SPONSORED OR SUPPORTED BY AN AGENCY OR ORGANIZATION OTHER THAN LAU, YOU REPRESENT THAT YOU HAVE FULFILLED ANY RIGHT OF REVIEW OR OTHER OBLIGATIONS REQUIRED BY SUCH CONTRACT OR AGREEMENT. LAU will clearly identify your name(s) as the author(s) or owner(s) of the submission, and will not make any alteration, other than as allowed by this license, to your submission.

Name: **Yara Zgheib**

Signature: 

Date: 20 / 06 / 2022
Day Month Year

LAU
الجامعة اللبنانية الأميركية
Lebanese American University

PLAGIARISM POLICY COMPLIANCE STATEMENT

I certify that:

1. I have read and understood LAU's Plagiarism Policy.
2. I understand that failure to comply with this Policy can lead to academic and disciplinary actions against me.
3. This work is substantially my own, and to the extent that any part of this work is not my own I have indicated that by acknowledging its sources.

Name: Yara Zgheib

Signature: 

Date: 20 / 06 / 2022
Day Month Year

To my Mathematical Family.

Acknowlegment

I wouldn't have made it this far, writing this thesis, without some individuals whom I'm grateful for and would like to deeply thank. First and foremost, I would like to express my gratitude towards Dr. Nader El Khatib. Knowing that he was not able to take on new students, he still decided to work with me and I am more than thankful for that. I also want to thank him for the continuous support and effort he provided me throughout this semester. Dr. El Khatib is, in my opinion, an exemplary Dr. and this for several reasons, from which I state: he always had the time to fully explain any inquiry I had, he was fully understanding and supportive and he never held back on widening my knowledge from the experience he has. Second, I would like to express my thanks to the respectful jury committee members, Dr. Chadi Nour and Dr. Jean Takchi. In addition, I want to thank my family who never left my side and always showed support in every decision that I made. Not to forget, my newly formed "family" consisting of my classmates with whom I spent the last 2 years, thank you for the help and the memories. Finally, I would also like to thank some of my friends, Elissa Salloum, Ghada Abi Younes and Lourdes Khalil who have helped me a lot and accompanied me throughout this whole thesis.

Effect of blood viscosity on the atherosclerotic plaque: A Fluid-Structure Interaction Model

Yara H. Zgheib

ABSTRACT

In this thesis, we study a fluid structure interaction problem between the blood and the atherosclerosis plaque formed inside an artery. The formation of this plaque may lead to dangerous consequences such as its rupture, the formation of blood clot that might result in a heart attack or an ischemic stroke. The blood is modeled as an incompressible non-Newtonian viscous fluid using the Navier-Stokes equations, the lipid pool and the fibrous cap of the atheroma plaque are supposed to be hyperelastic materials. The interactions between the blood (the fluid) and the plaque of atherosclerosis (the structure) are done after the Arbitrary Lagrangian Eulerian (ALE) method to handle employing the mesh displacement. In a stenosed artery, we investigate the hyperviscosity effects of blood on the blood flow of a COVID 19 patients, and the non-Newtonian one on the recirculation downstream of the atheroma plaque. After a mathematical analysis of the model, a finite element method is used to provide numerical simulations. The main interests of the numerical results are the displacement of the plaque, the distribution of the stress over it and the recirculation of the blood.

Simulations show that the Newtonian model where the viscosity is constant overestimates the recirculation of the blood, underestimates the displacement of the plaque and the stress over it in comparison with the non-Newtonian one. In addition, it shows also that the increase in the viscosity of the blood in a COVID

19 patient overestimates the distribution of the stress over the plaque that will lead to its rupture.

Keywords: Fluid Structure Interaction, viscosity, PDE, Mathematical Modeling, Numerical Simulations.

Table of Contents

List of Figures

List of Tables

Chapter 1

Introduction

1.1 Data collections

According to the World Health Organization, atherosclerotic cardiovascular disease (ASCVD) is the leading cause of mortality worldwide. Deaths from atherosclerosis represent 32% of the global deaths which consists of 18.56 million people dying each year [3]. For example, in Lebanon mortality related to cardiovascular diseases is 404.4 deaths per $100,000$ individuals, with an estimate of 45% of total death per year [4]. When looking at hospital records, the highest number of admissions was related to cardiovascular diseases, 30940 out of 37277 admissions in 2011 consisting mainly of older adults (60-65 years old) [5]. The most important complications associated with atherosclerosis are coronary heart disease and stroke. Taking into consideration all that was stated, it is important to understand the mechanism behind ASCVD as well as its effects on the individual's body.

1.2 The Biological Process

1.2.1 Blood

Before explaining the biological process of atherosclerosis and the formation of the plaque, we start by presenting the blood components (blood cells and plasma) and the main layers of the blood vessel wall structure.

Blood is a complex fluid that circulates in the heart, arteries, capillaries and veins, it absorbs the oxygen and transports it to different cells of body. The blood contains two main constituents: **blood cells** and **plasma**. The main blood cells, representing 45% of the total volume of the blood are [6]:

- Red Blood Cells (RBCs) also known as Erythrocytes that contain the haemoglobin protein. The main function is to transport the oxygen attracted by the haemoglobin to many cells and organs.
- White Blood Cells also known as Leucocytes, which have an important role in the defense mechanism of the body, protecting it by fighting off foreign bodies.
- Platelets or Thrombocytes, that help to regulate the blood flow and are responsible for blood coagulation when any part of the body is damaged [6].

The Plasma that represents 55% of the total volume of the blood contains 91.5% water and the remainder consists of proteins and other solutes [6].

The blood vessel whether it is the arteries or the veins consist of three main layers represented in figure (1.1):

- **Tunica Intima**: is the thinnest one it contains endothelial cells that form a single layer and it is in contact with blood flow.
- **Tunica Media**: it is made by smooth muscle, situated between the inner layer and the Tunica externa and its thickness differs between the arteries and the veins.

- **Tunica Externa**: elastic lamina that protect veins and arteries and encircles the Tunica Media.

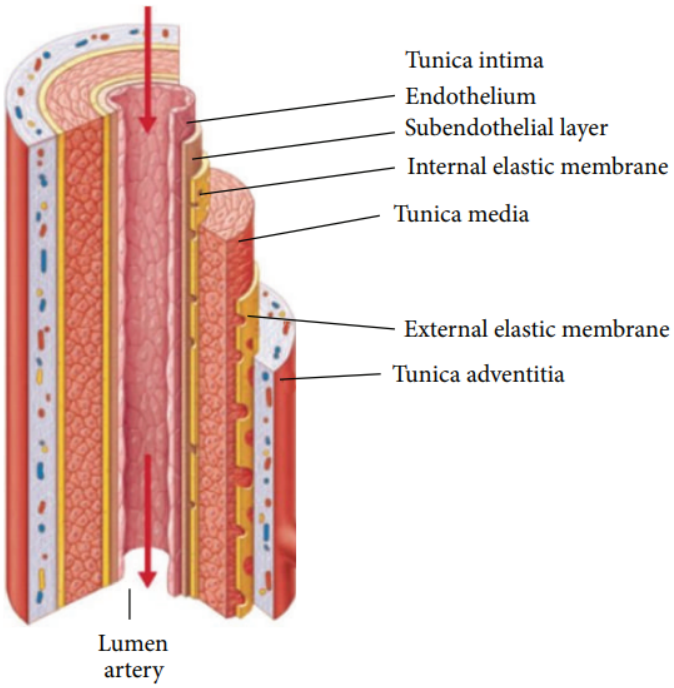

Figure 1.1: Blood vessel structure [1].

1.2.2 Definition of atherosclerosis

Atherosclerosis is a chronic inflammatory disease that may occur in arteries with a large or medium size. The abdominal aorta is rapidly affected followed by the coronary arteries. It is a buildup of fats, cholesterol and other substances called plaques within the artery wall. The atherosclerosis process begins by the inflammation: penetration of low density lipoprotein (LDL) into the intima where they are oxidized, then comes the lipid accumulation stage where the macrophages are transformed to foam cells, which is followed by the migration of smooth muscle cells over the lipid deposit that forms a fibrous plaque. This plaque modifies the blood flow, it can be degraded and can rupture due to several reasons.

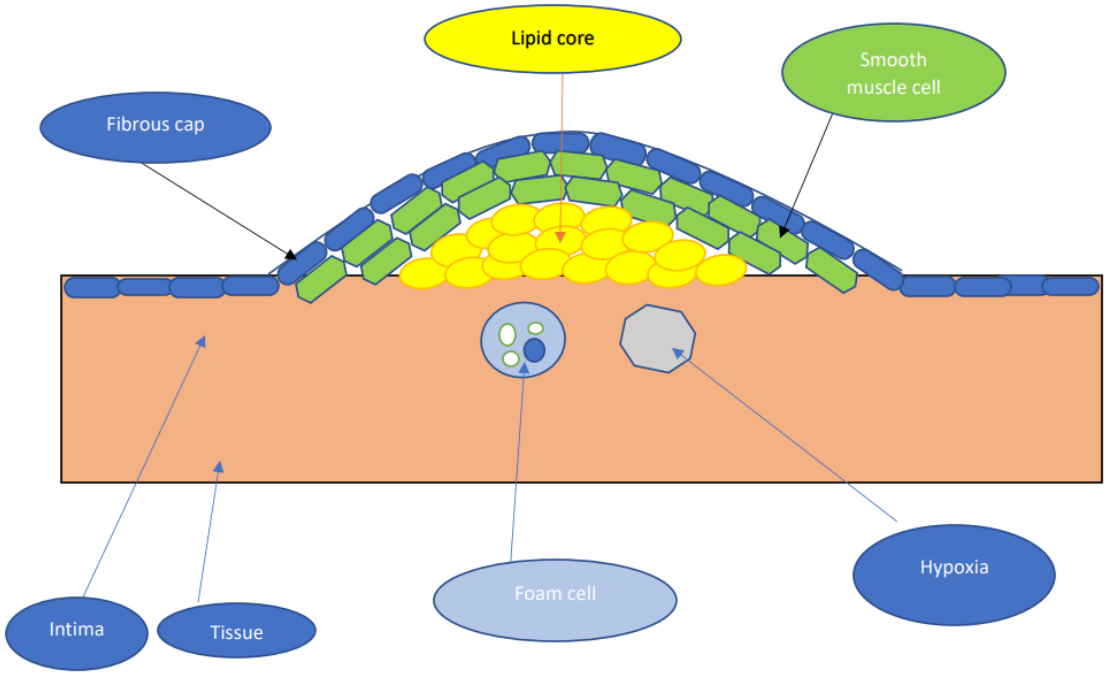

Figure 1.2: Plaque of atherosclerosis within the blood vessel

1.2.3 Risks Factors and Effects of Atherosclerosis

Several risk factors exist for atherosclerosis such as smoking, diabetes, obesity, family history, unhealthy diet rich in saturated and trans fat, high blood pressure as well as persistent elevations of triglycerides and cholesterol molecules in the body. The effects of atherosclerosis are:

- Atherosclerosis leads to a reduction in the artery lumen which will affect negatively on the blood circulation, reducing the amount of blood and oxygen that is delivered to vital organs including the heart and the brain.

- With time, the blood circulating in the arteries may lead to the rupture of the plaque. This will be followed by platelet recruitment and aggregation, as well as risk of stroke, thrombosis and cerebrovascular accident due to the clot burden that is traveling to the organs.

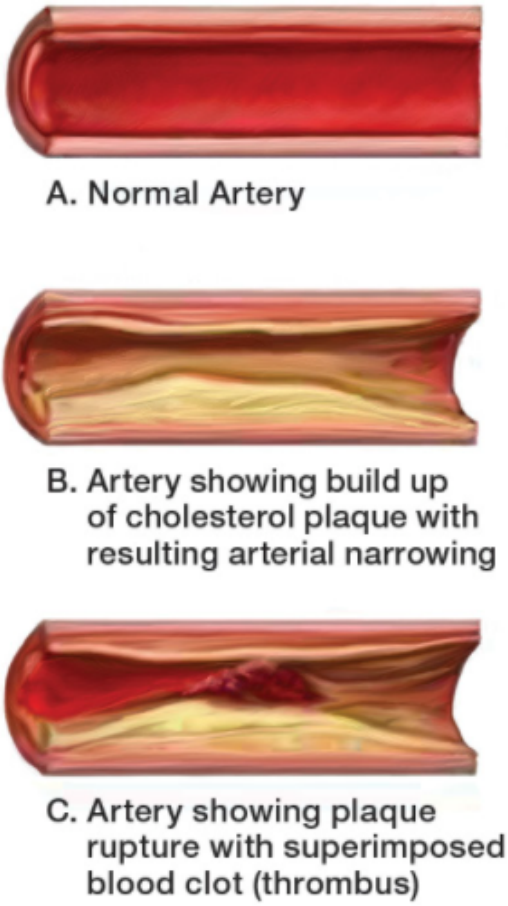

Figure 1.3: Effects of atherosclerosis on the artery. [2]

1.2.4 Blood viscosity

The viscosity of a fluid is a measure of its resistance to gradual deformation by stress. For example syrup has a higher viscosity than water and so it will have a lower velocity than water. The viscosity depends on a fluid's state, such as its temperature, pressure, and rate of deformation [7]. For the blood, the viscosity is one of the three basic determinants of its flow, it is an important factor that influences his rheology [8]. Blood viscosity is determined by plasma viscosity, hematocrit (volume fraction of red blood cell), red blood cell deformability and aggregation. The erythrocytes have the greatest effects on the viscosity, an increased number of red blood cells hematocrit will increase the viscosity and hence increase the resistance to the blood flow. So, factors involved in blood viscosity consist of the composition of the blood and the fats that circulate in the blood.

We can distinguish two types of fluids in term of viscosity either a Newtonian one where the viscosity is constant with respect to space, and the shear rate is directly proportional to the shear stress, or the Non Newtonian one where the viscosity is variable, can change under force and have a variable relationship with shear stress [9].

1.3 Fluid Structure Interaction in literature

In this section, we present various mathematical models of blood flow based on research studies on Fluid Structure Interaction.

- In paper [10], authors presented a mathematical model where they used the Navier Stokes equation to present the flow of the blood in the artery, and the generalized string model that governed the structure model. An ALE method is implemented in order to study this complex model. The aim of this paper is to analyze what is happening to a covid 19 patient where a rise of the blood viscosity occurred. After using a finite element method, a comparison was done between the results obtained from a normal viscosity condition and the hyper-viscous one. This model is solved by applying the fluid-structure interaction. A high velocity that leads to the thrombosis and low recirculation zones in the hyper-viscous model are the main results obtained at the end of the investigation.

- In paper [11], the point is to study the fluid structures interactions between the blood flow and the atherosclerotic plaque for a Newtonian and a Non-Newtonian model. Rupture of the plaque, recirculations of the blood that enhance the risk of clot formation that may result in a heart attack or an ischemic stroke are the main consequences of this interaction. The simulations demonstrate that Newtonian model overrates the recirculations, hence overrating the possibility of clot formation in comparison with the Non-Newtonian one. In addition, the Newtonian model where the viscosity

of the blood is constant underrates the Von Mises stress then the possibility of plaque rupture and this is expected because the viscosity for a Newtonian model is always inferior to the Non-Newtonian one.

- In [12], the authors proposed a coupled model which presents the blood as an incompressible non-Newtonian viscous fluid and the plaque of atherosclerotic treated as non linear hyperelastic is the solid model. The coupling of the fluid (blood) and the atherosclerotic plaque (solid) is obtained by an ALE method. They proved first the existence of a weak solution for an incompressible non-Newtonian fluid in a 2D study of the Navier-Stokes equations then they tested the model numerically. The results showed on the one hand that Newtonian and non-Newtonian model overrate the Von Mises stress over the plaque taking into consideration a rigid wall. On the other hand, with a compliant wall the non-Newtonian model underrates the stress over the atherosclerotic plaque and hence the possibility of plaque rupture. For the blood recirculations there is no difference between both models as well as between rigid and compliant wall.

Chapter 2

Mathematical Model and Analysis

2.1 Navier-Stokes equations

In this chapter, we take the blood as Newtonian fluid, with constant viscosity, as we will be working in large arteries. Blood flow is modeled using the Navier-Stokes equation, which describes its motion, coupled with the continuity equation. Taking into consideration some assumptions such as the blood flow is incompressible, no external forces are considered except the pressure gradient and that the atherosclerotic plaque is already formed, we get the following incompressible Navier-Stokes equation:

$$\frac{\partial \mathbf{u}}{\partial t} + (\mathbf{u}.\nabla)\mathbf{u} + \nabla p - 2\mathbf{div}(\nu \mathbf{D}(\mathbf{u})) = \mathbf{f} \text{ in } \Omega \ , \ t \in I \tag{2.1}$$

$$\text{div } \mathbf{u} = 0, \text{ in } \Omega, t \in I, \tag{2.2}$$

with $\mathbf{u} = \mathbf{u}_0$, in Ω, $t = t_0$, and:

- $\mathbf{u}$ is the blood flow velocity.

- p is the fluid pressure.
- $\mathbf{D(u)}$ refers to the strain rate.
- $\mathbf{f}$ represents external forces. In our study we consider $f = 0$.
- ν refers to the kinematic viscosity given by $\nu = \dfrac{\mu}{\rho}$ where μ is the dynamic viscosity and ρ is the density of the fluid.

Assuming that $0 < \nu_0 \leq \nu \leq \nu_1$ almost everywhere in Ω for all $t \in I$, then ν is a bounded strictly positive function.
The boundary conditions of this system of differential equations are:

$\mathbf{u} = \mathbf{g}$ on Γ^d, $t \in I$ (Dirichlet boundary)

$-p\mathbf{n} + 2\nu\mathbf{D(u)}.\mathbf{n} = \mathbf{h}$ on Γ^n, $t \in I$ (Neumann boundary)

where $\Gamma^d \cup \Gamma^n = \partial\Omega$.

2.1.1 Mathematical Analysis

The coupled problem is analyzed mathematically, we start by integrating over Ω the scalar product of the Navier-Stokes equation terms with a test function $\mathbf{v}$ to get the weak form. We obtain:

$$\int_\Omega (\frac{\partial \mathbf{u}}{\partial t} + (\mathbf{u}\cdot\nabla)\mathbf{u} + \nabla p - 2\ \mathrm{div}(\nu\mathbf{D(u)})) \cdot \mathbf{v}\ d\Omega$$

$$=(\tfrac{\partial \mathbf{u}}{\partial t}, \mathbf{v}) + ((\mathbf{u}\cdot\nabla)\mathbf{u}, \mathbf{v}) + \int_\Omega (\nabla p - 2\ \mathrm{div}(\nu\mathbf{D(u)})) \cdot \mathbf{v}\ d\Omega$$

By applying the Green integration formula [13], we obtain:

- $\displaystyle\int_\Omega \nabla p \cdot \mathbf{v} = -\int_\Omega \nabla\mathbf{v} \cdot p\ d\Omega + \int_{\partial\Omega} \mathbf{v}\cdot\mathbf{n}p\ d\partial\Omega,$

- $\int_\Omega -2\text{div}(\nu\mathbf{D}(\mathbf{u}))\cdot\mathbf{v}\ d\Omega$

$$= -2\int_\Omega \nu\mathbf{D}(\mathbf{u}):\mathbf{D}(\mathbf{v})\ d\Omega + \int_{\partial\Omega}\mathbf{v}\cdot(2\nu\mathbf{D}(\mathbf{u})\cdot\mathbf{n})\ d\partial\Omega.$$

So we get:

$$(\tfrac{\partial\mathbf{u}}{\partial t},\mathbf{v}) + ((\mathbf{u}\cdot\nabla)\mathbf{u},\mathbf{v}) + 2\int_\Omega \nu\mathbf{D}(\mathbf{u}):\mathbf{D}(\mathbf{v}) - (p,\text{div }\mathbf{v})$$

$$=\int_{\partial\Omega}\mathbf{v}\cdot(2\nu\mathbf{D}(\mathbf{u})\cdot\mathbf{n} - p\mathbf{n})\ d\partial\Omega$$

$\partial\Omega = \Gamma_d \cup \Gamma_n$ implies that:

$$\int_{\partial\Omega}\mathbf{v}\cdot(2\nu\mathbf{D}(\mathbf{u})\cdot\mathbf{n} - p\mathbf{n})\ d\partial\Omega = \int_{\Gamma^d}\mathbf{v}.(2\nu\mathbf{D}(\mathbf{u})\cdot\mathbf{n} - p\mathbf{n}) + \int_{\Gamma^n}\mathbf{v}\cdot\mathbf{h}$$

We assume that the Neumann boundary is given.

We choose $\mathbf{v}$ in $\mathbf{V} = \{\mathbf{v}\in H^1(\Omega) : \mathbf{v}|_{\Gamma^d} = 0\}$ so that we can eliminate the integral over Γ_d.

Similarly we multiply the continuity equation by a test function q belonging to a functional space Q, we obtain :

$$(div\mathbf{u}, q) = 0$$

We define Q by $\left\{q\in L^2(\Omega) : \text{with } \int_\Omega q = 0 \text{ if } \Gamma^d = \partial\Omega\right\}$ such that we can ensure the uniqueness of the pressure.

The velocity $\mathbf{u}$ belongs to $\mathbf{V}_g = \{\mathbf{u}\in H^1(\Omega) : \mathbf{u}|_{\Gamma^d} = \mathbf{g}\}$.

Hence the weak form of equations (2.1) and (2.2) reads:

$$\begin{cases} (\dfrac{\partial \mathbf{u}}{\partial t}, \mathbf{v}\ ) + a(\mathbf{u}, \mathbf{v}) + c(\mathbf{u}, \mathbf{u}, \mathbf{v}) + b(\mathbf{v}, p) = \displaystyle\int_{\Gamma^n} \mathbf{v} \cdot \mathbf{h}\ , \forall \mathbf{v} \in \mathbf{V}, \\ b(\mathbf{u}, q) = 0\ , \forall q \in Q, \end{cases} \tag{2.3}$$

where:

$$a(\mathbf{u}, \mathbf{v}) = 2 \int_\Omega \nu \mathbf{D}(\mathbf{u}) : \mathbf{D}(\mathbf{v}),$$

$$c(\mathbf{w}, \mathbf{u}, \mathbf{v}) = \int_\Omega ((\mathbf{w} \cdot \nabla)\mathbf{u}, \mathbf{v}),$$

$$b(\mathbf{v}, p) = -\int_\Omega p \text{ div } \mathbf{v}.$$

2.1.2 Homogeneous Dirichlet problem

In this part, we take $\partial\Omega = \Gamma^d$ and $\mathbf{g} = \mathbf{0}$. Therefore:

$$\mathbf{V} = \mathbf{H}_0^1(\Omega) = \left\{ \mathbf{v} \in H^1(\Omega) : \mathbf{v}|_{\partial\Omega} = 0 \right\},$$
$$Q = L_0^2(\Omega) = \left\{ q \in L^2(\Omega), \int_\Omega q = 0 \right\}.$$

The weak form gets to be:

$$\begin{cases} (\dfrac{\partial \mathbf{u}}{\partial t}, \mathbf{v}) + a(\mathbf{u}, \mathbf{v}) + c(\mathbf{u}, \mathbf{u}, \mathbf{v}) + b(\mathbf{v}, p) = 0\ , \forall \mathbf{v} \in \mathbf{V}, \\ b(\mathbf{u}, q) = 0\ , \forall q \in Q. \end{cases} \tag{2.4}$$

Proposition 2.1.1 *The bilinear forms $a : \boldsymbol{V} \times \boldsymbol{V} \to \mathbb{R}$ and $b : \boldsymbol{V} \times \boldsymbol{Q} \to \mathbb{R}$ and the trilinear form: $c : \boldsymbol{V} \times \boldsymbol{V} \times \boldsymbol{V} \to \mathbb{R}$ are continuous. The bilinear form $a(.,.)$ is also coercive that is $\exists \alpha > 0$ such that $a(\boldsymbol{v}, \boldsymbol{v}) \geq \alpha ||\boldsymbol{v}||^2_{\boldsymbol{H}^1(\Omega)}$, $\forall \boldsymbol{v} \in \boldsymbol{V}$.*

Proof

- *Continuity of $a(\boldsymbol{u}, \boldsymbol{v})$, $\forall \boldsymbol{u}, \boldsymbol{v} \in \boldsymbol{V}$:*

  Using Cauchy-Schwarz inequality [14], the equality: $||\boldsymbol{f}||^2_{\boldsymbol{H}^1(\Omega)} = ||\boldsymbol{f}||^2_{\boldsymbol{L}^2(\Omega)} + ||\nabla \boldsymbol{f}||^2_{\boldsymbol{L}^2(\Omega)}$ and $|\boldsymbol{v}|_{\boldsymbol{H}^1(\Omega)}$ is equivalent to the norm $||\boldsymbol{v}||_{\boldsymbol{H}^1(\Omega)}$ from Poincare's inequality [15]

we get:

$$\Big|a(\boldsymbol{u},\boldsymbol{v})\Big| = \Big|2\int_\Omega \nu \boldsymbol{D(u)} : \boldsymbol{D(v)}\Big| \leq \nu_1 \Big|\boldsymbol{D(u)}\Big|_2 \cdot \Big|\boldsymbol{D(v)}\Big|_2 \leq \nu_1 \Big|\boldsymbol{u}\Big|_{H^1(\Omega)} \Big|\boldsymbol{v}\Big|_{H^1(\Omega)}$$

$$\leq \nu_1 ||\boldsymbol{u}||_{H^1(\Omega)} ||\boldsymbol{v}||_{H^1(\Omega)}.$$

- *Continuity of* $b(\boldsymbol{u},p)$, $\forall \boldsymbol{u} \in \boldsymbol{V}$, $p \in Q$*:*
  $\Big|b(\boldsymbol{u},\boldsymbol{p})\Big| = \Big|\int_\Omega p\nabla\cdot\boldsymbol{u}\Big| \leq ||\nabla \boldsymbol{u}||_{L^2(\Omega)} \cdot ||p||_{L^2(\Omega)} \leq ||\boldsymbol{u}||_{H^1(\Omega)} ||p||_{L^2(\Omega)}.$

- *Continuity of* $c(\boldsymbol{w},\boldsymbol{u},\boldsymbol{v})$, $\forall \boldsymbol{w},\boldsymbol{u},\boldsymbol{v} \in \boldsymbol{V}$
  $\Big|c(\boldsymbol{w},\boldsymbol{u},\boldsymbol{v})\Big| = \Big|\int_\Omega (\boldsymbol{w}\cdot\nabla)\boldsymbol{u},\boldsymbol{v})\Big|$
  using the three-term Hölder inequality [15] $\forall p,q,r > 1$ *such that* $p^{-1}+q^{-1}+r^{-1} = 1$ *we get:*

$$\Big|\int_\Omega fghd\Omega\Big| \leq ||f||_{L^p(\Omega)} ||g||_{L^q(\Omega)} ||h||_{L^r(\Omega)}.$$

  So $\Big|c(\boldsymbol{w},\boldsymbol{u},\boldsymbol{v})\Big| = \Big|\int_\Omega ((\boldsymbol{w}\cdot\nabla)\boldsymbol{u},\boldsymbol{v})\Big| \leq ||\nabla\boldsymbol{w}||_{L^2(\Omega)} \cdot ||\boldsymbol{u}||_{L^4(\Omega)} \cdot ||\boldsymbol{v}||_{L^4(\Omega)}.$

  From Sobolev embedding theorem [15] $\boldsymbol{H}^1(\Omega) \hookrightarrow \boldsymbol{L}^6(\Omega)$ *as* $(N = 2,3)$ *and* $\boldsymbol{H}^1(\Omega) \hookrightarrow \boldsymbol{L}^4(\Omega)$*: if* $\boldsymbol{v} \in H^1(\Omega)$ *then* $||\boldsymbol{v}||_{L^4(\Omega)} \leq ||\boldsymbol{v}||_{H^1(\Omega)}$

  Hence
  $\Big|c(\boldsymbol{w},\boldsymbol{u},\boldsymbol{v})\Big| = \Big|\int_\Omega ((\boldsymbol{w}\cdot\nabla)\boldsymbol{u},\boldsymbol{v})\Big| \leq ||\nabla\boldsymbol{w}||_{L^2(\Omega)} \cdot ||\boldsymbol{u}||_{L^4(\Omega)} \cdot ||\boldsymbol{v}||_{L^4(\Omega)}$

  $$\leq C||\boldsymbol{w}||_{H^1(\Omega)}.||\boldsymbol{u}||_{H^1(\Omega)}.||\boldsymbol{v}||_{H^1(\Omega)}$$

- *Coercivity of* a, $\forall \boldsymbol{v} \in \boldsymbol{V}$*:*
  Using Poincare inequality and a consequence from the Korn inequality that may be found in CIARLET[1998], DUVAUT and LIONS[1976]:

$$a(\boldsymbol{v},\boldsymbol{v}) = \int_\Omega 2\nu \boldsymbol{D(v)} : \boldsymbol{D(v)} \geq 2\nu_0 \int_\Omega \boldsymbol{D(v)} : \boldsymbol{D(v)} \geq 2\nu_0 C_k ||\nabla \boldsymbol{v}||^2_{L^2(\Omega)}$$

$$\geq \tfrac{2\nu_0 C_k}{C_p^2} ||\boldsymbol{v}||^2_{L^2(\Omega)} \geq \alpha ||\boldsymbol{v}||^2_{H^1(\Omega)},\ \forall \boldsymbol{v} \in \boldsymbol{V}.$$

We define now the space $\mathbf{V}_{\text{div}} = \{\mathbf{v} \in \mathbf{V} : \nabla \cdot \mathbf{v} = 0 \text{ a.e in } \Omega\}$

Theorem 2.1.3 *$\boldsymbol{u}$ is a solution of the weak formulation (2.4) $\Rightarrow$ $\boldsymbol{u}(t) \in \boldsymbol{V}_{div}$ for all $t \in I$ and it satisfies*

$$(\frac{\partial \boldsymbol{u}}{\partial t}, \boldsymbol{v}) + a(\boldsymbol{u},\boldsymbol{v}) + c(\boldsymbol{u},\boldsymbol{u},\boldsymbol{v}) = 0,\ \forall \boldsymbol{v} \in \boldsymbol{V}_{div},\ t \in I. \tag{2.5}$$

Conversely, if, $\forall t \in I$, $\boldsymbol{u}(t) \in \boldsymbol{V}_{div}$ is a solution of (2.5) and $\frac{\partial u}{\partial t} \in \boldsymbol{L}^2(\Omega)$, then there exists a $!p \in Q$ such that $(\boldsymbol{u}, p)$ satisfies (2.4).

Proof

- *$\boldsymbol{u}$ is a solution of (2.4) $\Rightarrow b(\boldsymbol{u},q) = 0,\ \forall q \in Q \Rightarrow \int_\Omega q\ div\ \boldsymbol{u} = 0$*
  $\Rightarrow div\boldsymbol{u} = 0$
  so $\boldsymbol{u}$ belongs to $\boldsymbol{V}_{div}$ and $\boldsymbol{u}$ satisfies (2.5) $\forall \boldsymbol{v} \in \boldsymbol{V}_{div}, (b(\boldsymbol{v},p) = 0)$.

- *The second part of the proof of this theorem requires the result of the following lemma.*

  Lemma 2.1.5 *Let $\Omega \in \mathbb{R}^N$ and $L \in \boldsymbol{V'}$. Then $L(\boldsymbol{V}) = 0, \forall \boldsymbol{v} \in \boldsymbol{V}_{div}$ if and only if there exists a function $p \in L^2(\Omega)$ such that*

  $$L(v) = (p, div\boldsymbol{v}), \forall \boldsymbol{v} \in \boldsymbol{V}.$$

  Where $L(\boldsymbol{v}) = (\frac{\partial \boldsymbol{u}}{\partial t}, \boldsymbol{v}) + a(\boldsymbol{u},\boldsymbol{v}) + c(\boldsymbol{u},\boldsymbol{u},\boldsymbol{v}) - (\boldsymbol{f},\boldsymbol{v}),\ \forall \boldsymbol{v} \in \boldsymbol{V}$, belongs to $\boldsymbol{V'}$ being a linear continuous functional on $\boldsymbol{V}$.
  (Lemma 2.1 of GIRAULT and RAVIART [1986]).

  In our case $(\boldsymbol{f},\boldsymbol{v}) = 0$, $\boldsymbol{u}(t) \in \boldsymbol{V}_{div}$ is a solution of (2.5) so $L(\boldsymbol{V}) = 0, \forall \boldsymbol{v} \in \boldsymbol{V}_{div}$. By lemma (2.1.5), there exists a function $p \in L^2(\Omega)$ such that $L(\boldsymbol{v}) = (p, div\boldsymbol{v}), \forall \boldsymbol{v} \in \boldsymbol{V}$ so $(\frac{\partial \boldsymbol{u}}{\partial t}, \boldsymbol{v}) + a(\boldsymbol{u},\boldsymbol{v}) + c(\boldsymbol{u},\boldsymbol{u},\boldsymbol{v}) = (p, div\boldsymbol{v}) = -b(\boldsymbol{v},p),\ \forall \boldsymbol{v} \in \boldsymbol{V}$ so $(\boldsymbol{u},p)$ satisfies (2.4) hence we obtain the desired result.

Lemma 2.1.6 *If $\boldsymbol{u}$ is a solution of system (2.4) thus $c(\boldsymbol{u},\boldsymbol{u},\boldsymbol{u})=0$.*

Proof $c(\boldsymbol{u},\boldsymbol{u},\boldsymbol{u})=\int_\Omega(\boldsymbol{u}\cdot\nabla)\boldsymbol{u}\cdot\boldsymbol{u}=\int_\Omega\frac{1}{2}\nabla(|\boldsymbol{u}|^2)\cdot\boldsymbol{u}=-\frac{1}{2}\int_\Omega|\boldsymbol{u}|^2 div\ \boldsymbol{u}+\frac{1}{2}\int_\Omega|\boldsymbol{u}|^2\boldsymbol{u}\cdot\boldsymbol{n}$ *(from Green's formula).*

Taking $\boldsymbol{u}|_{\partial\Omega}=0$, we get $\int_\Omega\boldsymbol{u}\cdot\boldsymbol{n}=0$ and $\int_\Omega div\ \boldsymbol{u}=0$.

$c(\boldsymbol{u},\boldsymbol{u},\boldsymbol{u})=-\frac{1}{2}\int_\Omega\left|\boldsymbol{u}\right|^2 div\ \boldsymbol{u}=-\frac{1}{2}\int_\Omega\left|\boldsymbol{u}\right|^2 div\ \boldsymbol{u}+\frac{\boldsymbol{c}}{2}\int_\Omega div\ \boldsymbol{u}$

with $\boldsymbol{c}=\int_\Omega\left|\boldsymbol{u}\right|^2$,

$c(\boldsymbol{u},\boldsymbol{u},\boldsymbol{u})=-\frac{1}{2}(\int_\Omega(\left|\boldsymbol{u}\right|^2-\boldsymbol{c})div\ \boldsymbol{u})=-\frac{1}{2}\ b(\boldsymbol{u},(\left|\boldsymbol{u}\right|^2-\boldsymbol{c}))=0.$

as $(|\boldsymbol{u}|^2-\boldsymbol{c})\in Q$ and $b(\boldsymbol{u},q)=0,\forall q\in Q$ ($\boldsymbol{u}$ is a solution of (2.4)).

Theorem 2.1.8 *Let $\boldsymbol{u}(t)\in\boldsymbol{V}_{div}$ be a solution of (2.4) Then:*

$$||\boldsymbol{u}(t)||^2_{L^2(\Omega}+\boldsymbol{C}_1\int_0^t||\nabla\boldsymbol{u}(\tau)||^2_{L^2(\Omega}d\tau\leq e^t(||\boldsymbol{u}_0||^2_{L^2(\Omega)}) \tag{2.6}$$

where $\boldsymbol{C}_1=4\mu_0C_k$, and

$$||\boldsymbol{u}(t)||^2_{L^2(\Omega}+\boldsymbol{C}_2\int_0^t||\nabla\boldsymbol{u}(\tau)||^2_{L^2(\Omega}d\tau\leq||\boldsymbol{u}_0||^2_{L^2(\Omega)} \tag{2.7}$$

where $\boldsymbol{C}_2=2\mu_0C_k$, $\boldsymbol{C}_k$ is the constant of Korn inequality.

(2.6) and (2.7) are the energy inequalities for the Navier-Stokes equation.

Proof *$\forall u\in\boldsymbol{V}_{div}$, we take $\boldsymbol{v}$=$\boldsymbol{u}(t)$ in equation (2.5). Then*

$$\frac{1}{2}\frac{d}{dt}||\boldsymbol{u}(t)||^2_{L^2(\Omega)}+c(\boldsymbol{u},\boldsymbol{u},\boldsymbol{u})+a(\boldsymbol{u},\boldsymbol{u})=0$$

From lemma (2.1.6), $c(\boldsymbol{u},\boldsymbol{u},\boldsymbol{u})$=0 $\implies$ $\frac{1}{2}\frac{d}{dt}||\boldsymbol{u}(t)||^2_{L^2(\Omega)}+a(\boldsymbol{u},\boldsymbol{u})=0$
In addition $a(\boldsymbol{u},\boldsymbol{u})=2\int_\Omega\nu\boldsymbol{D}(\boldsymbol{u}):\boldsymbol{D}(\boldsymbol{u})\geq 2\mu_0\boldsymbol{C}_k||\nabla\boldsymbol{u}(t)||^2_{L^2(\Omega)}$ using Korn inequality result.

Then,

$$\frac{d}{dt}||\boldsymbol{u}(t)||^2_{L^2(\Omega)}+4\mu_0\boldsymbol{C}_k||\nabla\boldsymbol{u}(t)||^2_{L^2(\Omega)} \leq \frac{d}{dt}||\boldsymbol{u}(t)||^2_{L^2(\Omega)}+2a(\boldsymbol{u},\boldsymbol{u}) = 0 \leq 2\epsilon||\boldsymbol{u}(t)||^2_{L^2(\Omega)}$$

for all $\epsilon > 0$.

Choosing $\epsilon = 0.5$ *and integrating between* t_0 *and* t *we get:*

$$||\boldsymbol{u}||^2_{L^2(\Omega)} + 4\mu_0\boldsymbol{C}_k\int_{t_0}^{t}||\nabla\boldsymbol{u}||^2_{L^2(\Omega)}d\tau \leq \int_{t_0}^{t}||\boldsymbol{u}||^2_{L^2(\Omega)} + ||\boldsymbol{u}_0||^2_{L^2(\Omega)}$$

By applying Gronwall's lemma [16] and considering:

$$||\boldsymbol{u}||^2_{L^2(\Omega)} + 4\mu_0\boldsymbol{C}_k\int_{t_0}^{t}||\nabla\boldsymbol{u}||^2_{L^2(\Omega)}d\tau \text{ as } \phi(t)$$

We obtain:

$$||\boldsymbol{u}||^2_{L^2(\Omega)} + 4\mu_0\boldsymbol{C}_k\int_{t_0}^{t}||\nabla\boldsymbol{u}||^2_{L^2(\Omega)}d\tau \leq ||\boldsymbol{u}_0||^2_{L^2(\Omega)}e^t.$$

for $\boldsymbol{C}_1 = 4\mu_0 C_k$ *we get the first inequality.*

For the second inequality, we use the following:

$$\frac{d}{dt}||\boldsymbol{u}(t)||^2_{L^2(\Omega)} + 4\mu_0\boldsymbol{C}_k||\nabla\boldsymbol{u}(t)||^2_{L^2(\Omega)} \leq 0 \leq 2\epsilon||\boldsymbol{u}(t)||^2_{L^2(\Omega)}$$

Using the Poincare inequality, we get:

$$\frac{d}{dt}||\boldsymbol{u}(t)||^2_{L^2(\Omega)} + 4\mu_0\boldsymbol{C}_k||\nabla\boldsymbol{u}(t)||^2_{L^2(\Omega)} \leq 0 \leq 2\epsilon||\boldsymbol{u}(t)||^2_{L^2(\Omega)} \leq 2\epsilon\boldsymbol{C}_p^2||\nabla\boldsymbol{u}(t)||^2_{L^2(\Omega)}$$

Choosing $\epsilon = \frac{\mu_0\boldsymbol{C}_k}{\boldsymbol{C}_p^2}$ *and integrating between* t_0 *and* t *we obtain:*

$$||\boldsymbol{u}||^2_{L^2(\Omega)} + 4\mu_0\boldsymbol{C}_k\int_{t_0}^{t}||\nabla\boldsymbol{u}||^2_{L^2(\Omega)}d\tau \leq \frac{2\mu_0\boldsymbol{C}_k\boldsymbol{C}_p^2}{\boldsymbol{C}_p^2}||\nabla\boldsymbol{u}(t)||^2_{L^2(\Omega)} + ||\boldsymbol{u}_0||^2_{L^2(\Omega)}$$

$$||\boldsymbol{u}(t)||^2_{L^2(\Omega} + 2\mu_0 \boldsymbol{C}_k \int_0^t ||\nabla \boldsymbol{u}(\tau)||^2_{L^2(\Omega} d\tau \leq ||\boldsymbol{u}_0||^2_{L^2(\Omega)}$$

for $\boldsymbol{C}_2 = 2\mu_0 C_k$*, hence we prove the second inequality.*

2.2 Generalized string model

The generalized string model takes into consideration the effects of the longitudinal stresses σ_z, we add this assumption to the independent ring model [15] assumptions and we get this form:

$$\frac{\partial^2 \eta}{\partial t^2} - a\frac{\partial^2 \eta}{\partial z^2} + b\eta - c\frac{\partial^3 \eta}{\partial t \partial z^2} = H, \text{ in } \Gamma_0^w,\ t \in I \tag{2.8}$$

where:

$\eta = \eta_0$, $\frac{\partial \eta}{\partial t} = \eta_1$ in Γ_0^w, $t = t_0$

$\eta|_{z=0} = \alpha$, $\eta|_{z=L} = \beta$, $t \in I$.

Γ_0^w is the reference configuration.

In our study H is equal to 0, no external forces are considered.

We define:

$e_s(t) = \frac{1}{2}\left(\left|\left| \frac{\partial \eta}{\partial t}(t) \right|\right|^2_{L^2(\Gamma_0^w)} + a \left|\left| \frac{\partial \eta}{\partial z}(t) \right|\right|^2_{L^2(\Gamma_0^w)} + b \left|\left| \eta(t) \right|\right|^2_{L^2(\Gamma_0^w)} \right)$ the energy function.

Lemma 2.2.1 *For* $H = \alpha = \beta = 0$ *for a.e* $t \in I$*:*

$$e_s(t) + c \int_{t_0}^t \left|\left| \frac{\partial^2 \eta}{\partial t \partial z}(\tau) \right|\right|^2_{L^2(\Gamma_0^w)} d\tau \leq e_s(0) \tag{2.9}$$

where C_p is the Poincare constant.

Proof *First, we multiply (2.8) by $\frac{\partial \eta}{\partial t}$ and we integrate with respect to z:*

$$\int_0^L \frac{\partial \eta}{\partial t}\frac{\partial^2 \eta}{\partial t^2} - a\int_0^L \frac{\partial \eta}{\partial t}\frac{\partial^2 \eta}{\partial z^2} + b\int_0^L \frac{\partial \eta}{\partial t}\eta - c\int_0^L \frac{\partial \eta}{\partial t}\frac{\partial^3 \eta}{\partial t \partial z^2}$$

$$= \frac{1}{2}\frac{d}{dt}\int_0^L (\frac{\partial \eta}{\partial t})^2 + a\int_0^L \frac{\partial \eta}{\partial z}\frac{\partial^2 \eta}{\partial z \partial t} - a\Big[\frac{\partial \eta}{\partial t}\frac{\partial \eta}{\partial z}\Big]_0^L + \frac{b}{2}\frac{d}{dt}\int_0^L \eta^2 + c\int_0^L \Big(\frac{\partial^2 \eta}{\partial t \partial z}\Big)^2 - c\Big[\frac{\partial^2 \eta}{\partial t \partial z}\frac{\partial \eta}{\partial t}\Big]_0^L$$

$$= 0$$

we have: $\frac{\partial^2 \eta}{\partial t \partial z}\frac{\partial \eta}{\partial z} = \frac{1}{2}\frac{\partial}{\partial t}(\frac{\partial \eta}{\partial z})^2$ and by applying the homogeneous boundary conditions, we obtain:

$$\frac{1}{2}\frac{d}{dt}\int_0^L (\frac{\partial \eta}{\partial t})^2 + \frac{a}{2}\frac{d}{dt}\int_0^L \frac{\partial \eta^2}{\partial z} + \frac{b}{2}\frac{d}{dt}\int_0^L \eta^2 + c\int_0^L \Big(\frac{\partial^2 \eta}{\partial t \partial z}\Big)^2 = 0$$

then

$$\frac{de_s}{dt} + c\left|\left|\frac{\partial^2 \eta}{\partial t \partial z}\right|\right|^2_{L^2(\Gamma_0^w)} = 0.$$

Integrating between t_0 and t we get the desired result.

2.3 Fluid-Structure interaction

In this section, we study the fluid structure interaction between the blood and the plaque of atherosclerosis in large arteries where the vessel wall may vary up to 10% [17]. For coupling the fluid-structure problem, we use the generalized string model for the structure considered as a hyperelastic material and the Navier-Stokes equation for the blood. On the interface where the interaction between the blood and the plaque of atherosclerosis occurs, we take into consideration two conditions:

- Continuity of velocity.
- Mechanical equilibrium.

This is explained in figure (2.1).

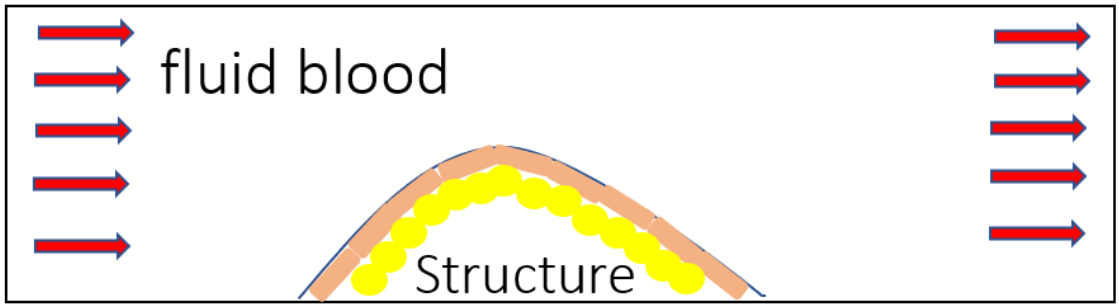

Figure 2.1: A 2D domain for the blood vessel where the plaque of atherosclerosis is formed.

2.3.1 The arbitrary Lagrangian Eulerian method

The arbitrary Lagrangian Eulerian (ALE) method connects a Lagrangian and Eulerian approach together through the velocity of the mesh. In our case, the Navier-Stokes equation for the fluid is treated as Eulerian. For the solid, where the domain is moving under the effect of the flow field, the Lagrangian approach is more practical. However, the inlet and outlet boundaries will be transported along the fluid trajectories that lead to a distortion of the domain. A part of the domain of the fluid will take a part of the domain of the structure and vice versa. So we introduce the Arbitrary Lagrangian Eulerian mapping:

$$\mathcal{A}_t : \Omega_0 \to \Omega_{\mathcal{A}_t},\ \mathbf{Y} \to \mathbf{y}(t, \mathbf{Y}) = \mathcal{A}_t(\mathbf{Y}),\ \Omega_{\mathcal{A}_t} \equiv \mathcal{A}_t(\Omega_0) = \Omega_t,\ \forall t \in I$$

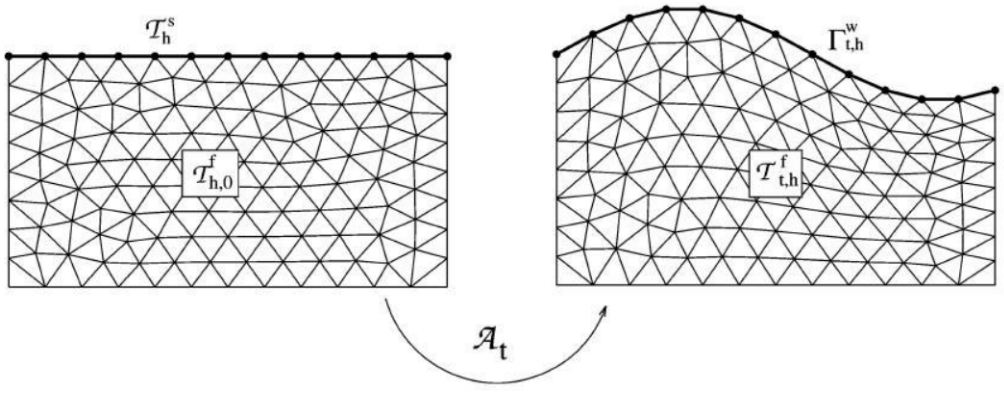

Figure 2.2: $\mathcal{A}_t$ is a mapping from the old mesh to the new one where the deformations occurs on the boundaries [15].

From the ALE mapping we may define the domain velocity field as:

$\tilde{\mathbf{w}}(t, \mathbf{Y}) = \frac{\partial}{\partial t}\mathbf{y}(t, \mathbf{Y})$, then $\mathbf{w} = \tilde{\mathbf{w}} \circ \mathcal{A}_t^{-1}$ i.e $\mathbf{w}(t, \mathbf{Y}) = \tilde{\mathbf{w}}(t, \mathcal{A}_t^{-1}(\mathbf{y}))$.

We indicate by $\tilde{f}$ the composition of a function f with the ALE mapping:

$$\tilde{f} = f \circ \mathcal{A}_t.$$

The ALE derivative of a function f is denoted by $\frac{D^{\mathcal{A}}}{Dt} f$, where:

$$f : I \times \Omega_t \to \mathbb{R}, \text{ and } \frac{D^{\mathcal{A}}}{Dt} f : I \times \Omega_t \to \mathbb{R}.$$

So we have $\frac{D^{\mathcal{A}}}{Dt} f = \frac{\partial f}{\partial t} + \mathbf{w} \cdot \nabla f$.

We put into evidence the ALE time derivative for the Navier-Stokes equation and we get:

$$\frac{D^{\mathcal{A}}}{Dt}\mathbf{u} + [(\mathbf{u} - \mathbf{w}) \cdot \nabla]\mathbf{u} + \nabla p - 2\text{div}(\nu \mathbf{D}(\mathbf{u})) = 0, \tag{2.10}$$

$$\text{div } \mathbf{u} = 0, \text{ in } \Omega_t, \forall t \in I. \tag{2.11}$$

2.3.2 Mathematical model

The coupled fluid-structure problem using the generalized string model for the structure, the equations (2.10) and (2.11) for the blood is:

$$\begin{cases} \dfrac{D^{\mathcal{A}}}{Dt}\mathbf{u} + [(\mathbf{u} - \mathbf{w}) \cdot \nabla]\mathbf{u} + \nabla p - 2\mathbf{div}(\nu \mathbf{D}(\mathbf{u})) = 0, \text{ with div } \mathbf{u} = 0, \text{ in } \Omega_t \\ \dfrac{\partial^2 \eta}{\partial t^2} - a\dfrac{\partial^2 \eta}{\partial z^2} + b\eta - c\dfrac{\partial^3 \eta}{\partial t \partial z^2} = 0, \text{ in } \Gamma_0^w. \end{cases} \tag{2.12}$$

With the following initial conditions for $t = t_0$:

$$\mathbf{u} = \mathbf{u}_0, \, x \in \Omega_0, \, \eta = \eta_0, \, \dot{\eta} = \eta_1, \text{ in } \Gamma_0^w,$$

boundary conditions for $t \in I$,

$$[2\nu \mathbf{D}(\mathbf{u}) - (p - P_{ext})\mathbf{I}].\mathbf{n} = 0, \text{ on } \Gamma_t^{out},$$

$$\mathbf{u} = \mathbf{g}, \text{ on } \Gamma_t^{in}, \ \eta|_{z=0} = \alpha, \ \eta|_{z=L} = \beta,$$

and the interface condition:

$$\tilde{\mathbf{u}} = \mathbf{u} \circ \mathcal{A}_t = \frac{\partial \eta}{\partial t}\mathbf{e}_r, \text{ on } \Gamma_0^w, \ t \in I.$$

2.3.3 Energy inequality

In this part, we will consider the case of homogeneous boundary conditions to get an energy inequality for the coupled problem just presented.
We take $\mathbf{g} = 0$ and $\alpha = \beta = 0$.

Lemma 2.3.1 *The coupled problem just presented with the homogeneous boundary conditions satisfies the following equality for all $t \in I$:*
$$\frac{d}{dt}\left[\frac{w}{2}||\boldsymbol{u}(t)||_{L^2(\Omega_t)} + e_s(t)\right] + 2w\int_{\Omega_t} \nu \boldsymbol{D(u)} : \boldsymbol{D(u)} + \left|\left|\frac{\partial^2 \eta}{\partial z \partial t}\right|\right|^2_{L^2(\Gamma_0^w)} + \frac{w}{2}\int_{\Gamma_t^{out}} |\boldsymbol{u}|^2 \boldsymbol{u.n} = 0$$

where e_s was defined before and $w = \frac{\rho}{\rho_w h_0}$.

In addition, if we assume: $\int_{\Gamma_t^{out}} |\boldsymbol{u}|^2 \boldsymbol{u.n} \geq 0$, $\forall t \in I$ [15], we get the a-priori energy estimate:
$$\frac{w}{2}||\boldsymbol{u}(t)||_{L^2(\Omega_t)} + e_s(t) + C_k w \nu_0 \int_{t_0}^t ||\nabla \boldsymbol{u}||^2_{L^2(\Omega_\tau)} d\tau + c\int_{t_0}^t \left|\left|\frac{\partial^2 \eta}{\partial z \partial t}\right|\right|^2_{L^2(\Gamma_0^w)} d\tau$$
$$\leq \frac{w}{2}||\boldsymbol{u}_0||_{L^2(\Omega_t)} + e_s(t_0) \ \forall t \in I.$$

Proof *First, we multiply the equation (2.10) by $\boldsymbol{u}$. Secondly, we integrate over Ω_t, we obtain:*

$$\int_{\Omega_t} \boldsymbol{u} \cdot \frac{D^{\mathcal{A}}}{Dt}\boldsymbol{u} + \int_{\Omega_t} \boldsymbol{u} \cdot [(\boldsymbol{u}-\boldsymbol{w}) \cdot \nabla]\boldsymbol{u} + \int_{\Omega_t} \boldsymbol{u} \cdot (\nabla p - 2\nu div\ \boldsymbol{D(u)}) = 0.$$

By applying the ALE transport theorem [15], we obtain:

$$\int_{\Omega_t} \boldsymbol{u} \cdot \frac{D^{\mathcal{A}}}{Dt}\boldsymbol{u} = \frac{1}{2}\frac{d}{dt}\int_{\Omega_t} |\boldsymbol{u}|^2 - \frac{1}{2}\int_{\Omega_t} |\boldsymbol{u}|^2 div\ \boldsymbol{w}.$$

For the second term, by applying Green formula we obtain:

$$\begin{aligned}\int_{\Omega_t} \boldsymbol{u} \cdot [(\boldsymbol{u}-\boldsymbol{w}) \cdot \nabla]\boldsymbol{u} &= \frac{1}{2}\int_{\Omega_t} \nabla\Big|\boldsymbol{u}\Big|^2 \cdot (\boldsymbol{u}-\boldsymbol{w}) \\ &= -\tfrac{1}{2}\int_{\Omega_t} |\boldsymbol{u}|^2 div\ \boldsymbol{u} + \frac{1}{2}\int_{\Omega_t} |\boldsymbol{u}|^2 div\ \boldsymbol{w} + \frac{1}{2}\int_{\partial\Omega_t} |\boldsymbol{u}|^2 (\boldsymbol{u}-\boldsymbol{w}) \cdot \boldsymbol{n} \\ &= \tfrac{1}{2}\int_{\Omega_t} |\boldsymbol{u}|^2 div\ \boldsymbol{w} + \frac{1}{2}\int_{\Gamma_t^{out}} |\boldsymbol{u}|^2 \boldsymbol{u} \cdot \boldsymbol{n}.\end{aligned}$$

(since div $\boldsymbol{u} = 0$ *and* $\boldsymbol{w} = 0$ *on* $\partial\Omega_t \setminus \Gamma_t^w$*.)*

For the others terms we apply also Green formula and we obtain:

$$\begin{aligned}\int_{\Omega_t} \boldsymbol{u} \cdot \nabla p &= \int_{\Omega_t} \boldsymbol{u} \cdot \nabla(p - p_{ext})\ (p_{ext}\ \textit{is constant}) \\ &= -\int_{\Omega_t} (p - p_{ext}) div\ \boldsymbol{u} + \int_{\partial\Omega_t} (p - p_{ext}) \cdot \boldsymbol{u} \cdot \boldsymbol{n} \\ &= \int_{\Gamma_t^{out}} (p - p_{ext}) \cdot \boldsymbol{u} \cdot \boldsymbol{n} + \int_{\Gamma_t^{w}} (p - p_{ext}) \cdot \boldsymbol{u} \cdot \boldsymbol{n}\end{aligned}$$

and

$$\begin{aligned}\int_{\Omega_t} \nu\boldsymbol{u} \cdot \boldsymbol{div D(u)} &= -\int_{\Omega_t} \nu\nabla\boldsymbol{u} : \boldsymbol{D(u)} + \int_{\partial\Omega_t} \nu\boldsymbol{u} \cdot \boldsymbol{D(u)} \cdot \boldsymbol{n} \\ &= -\int_{\Omega_t} \nu\boldsymbol{D(u)} : \boldsymbol{D(u)} + \int_{\partial\Omega_t} \nu\boldsymbol{u} \cdot \boldsymbol{D(u)} \cdot \boldsymbol{n}\end{aligned}$$

$$= -\int_{\Omega_t} \nu \boldsymbol{D(u)} : \boldsymbol{D(u)} + \int_{\Gamma_t^{out}} \nu(\boldsymbol{D(u)} \cdot \boldsymbol{n}) \cdot \boldsymbol{u} + \int_{\Gamma_t^{w}} \nu(\boldsymbol{D(u)} \cdot \boldsymbol{n}) \cdot \boldsymbol{u}$$

Using these results and the boundary conditions we can write:

$$\frac{1}{2}\frac{d}{dt}||\boldsymbol{u}||^2_{L^2(\Omega_t)} + 2\int_{\Omega_t} \nu \boldsymbol{D(u)} : \boldsymbol{D(u)} + \frac{1}{2}\int_{\Gamma_t^{out}} |\boldsymbol{u}|^2 \boldsymbol{u} \cdot \boldsymbol{n}$$

$$+ \int_{\Gamma_t^{w}} \Big[(p - p_{ext})n - 2\nu \boldsymbol{D(u)} \cdot \boldsymbol{n}\Big] \cdot \boldsymbol{u} = 0$$

We add this equality multiplied by w to the result of lemma (2.2.1) we obtain the first result.

Using this result, the inequality: $\int_{\Gamma_t^{out}} |\boldsymbol{u}|^2 \boldsymbol{u}.\boldsymbol{n} \geq 0$, $\forall t \in I$, *the fact that* $\nu \geq \nu_0 > 0$, *the Poincare inequality we get the desired result.*

Chapter 3

Numerical Simulations

We consider the blood vessel as a rectangular domain with an atheromatous plaque in his lumen. The blood flow is modeled as Newtonian fluid governed by these equations (2.1) and (2.2) for incompressible fluids.

The values of parameters for the Newtonian model are taken from table (3.1). The atheromatous plaque formed by the fibrous cap and the lipid pool is modeled as isotropic nearly incompressible hyperelastic materials. According to the Mooney-Rivlin model the values of parameters are chosen for the energy function and are taken from table (3.1).

Parameters	**Values**	**References**
Fluid: Blood		
Density	$1060Kg/m^3$	[12]
Viscosity	0.0035 Pa s	[18]
Hyper-Viscosity	0.0042 Pa s	[19]
Fibrous cap		
c_{10}	$9200N.m^{-2}$	[20]
c_{01}	0	[20]
κ	$3e^9$ Pa	[20]
Density	$1000Kg.m^{-2}$	[20]
Lipid Pool		
c_{10}	$500N.m^{-2}$	[20]
c_{01}	0	[20]
κ	200 MPa	[20]
Density	$1000Kg.m^{-2}$	[20]

Table 3.1: Choice of Parameters.

In addition, we take into consideration the blood flow modeled as a non-Newtonian fluid in our simulations. We consider μ the viscosity determined by the Carreau law given by:

$$\mu = \mu_\infty + (\mu_0 - \mu_\infty)(1 + \lambda s(u))^2)^{(n-1)/2}$$

The values of parameters for the non-Newtonian model are taken from table (3.2).

Parameters	**Values**	**References**
Fluid: Blood		
Zero shear rate limit (μ_0)	0.056 Pa.s	[21]
Infinite shear rate limit (μ_∞)	0.0035 Pa s	[21]
Relaxation time-constant (λ)	3.313 s	[21]
Power low index in Carreau model (n)	0.3568	[21]

Table 3.2: Parametric values for the non-Newtonian model.

We perform the simulations using COMSOL Multiphysics, and we export the total displacement, Von Mises stress for every case in many times.

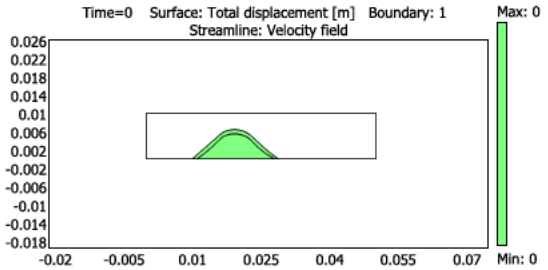

Figure 3.1: Total displacement of the plaque with a constant viscosity (μ = 0.0035) at t=0.

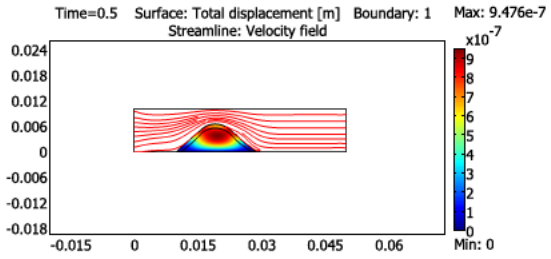

Figure 3.2: Total displacement of the plaque with a constant viscosity (μ = 0.0035) at t=0.5.

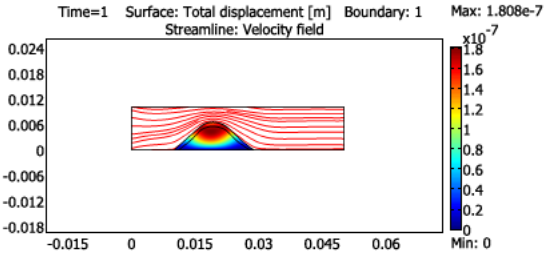

Figure 3.3: Total displacement of the plaque with a constant viscosity (μ = 0.0035) at t=1.

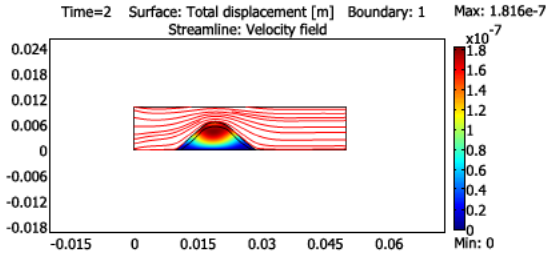

Figure 3.4: Total displacement of the plaque with a constant viscosity (μ = 0.0035) at t=2.

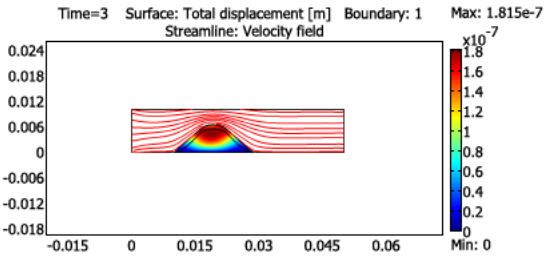

Figure 3.5: Total displacement of the plaque with a constant viscosity (μ = 0.0035) at t=3.

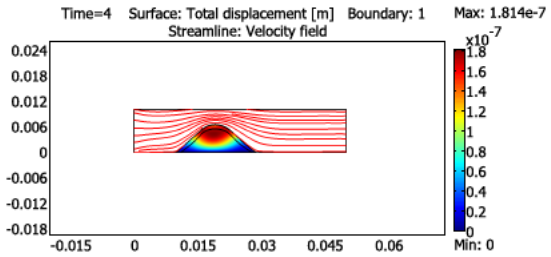

Figure 3.6: Total displacement of the plaque with a constant viscosity (μ = 0.0035) at t=4.

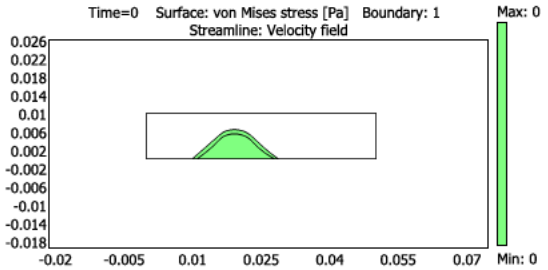

Figure 3.7: The stress over the plaque with a constant viscosity ($\mu = 0.0035$) at t=0

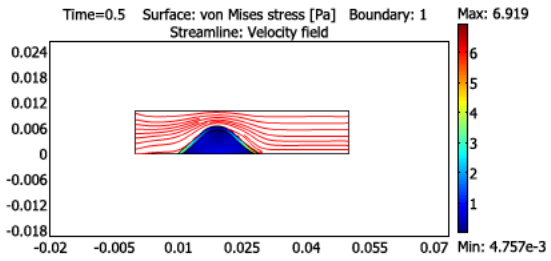

Figure 3.8: The stress over the plaque with a constant viscosity ($\mu = 0.0035$) at t=0.5.

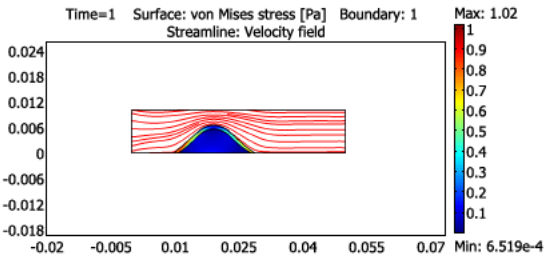

Figure 3.9: The stress over the plaque with a constant viscosity ($\mu = 0.0035$) at t=1.

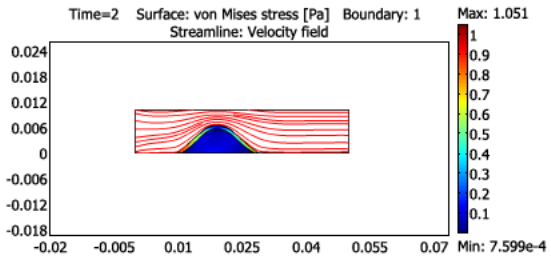

Figure 3.10: The stress over the plaque with a constant viscosity ($\mu = 0.0035$) at t=2.

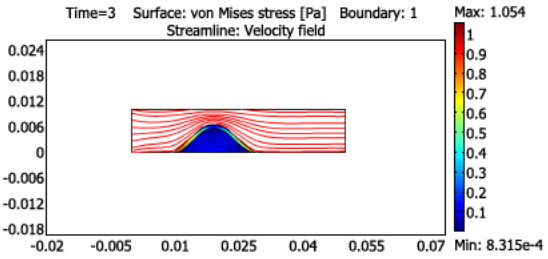

Figure 3.11: The stress over the plaque with a constant viscosity ($\mu = 0.0035$) at t=3.

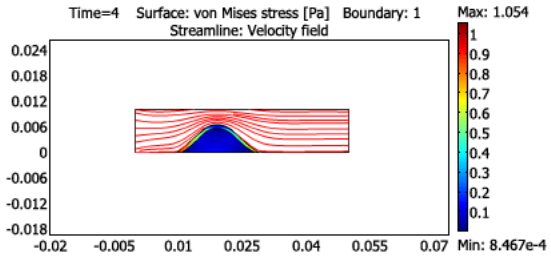

Figure 3.12: The stress over the plaque with a constant viscosity ($\mu = 0.0035$) at t=4.

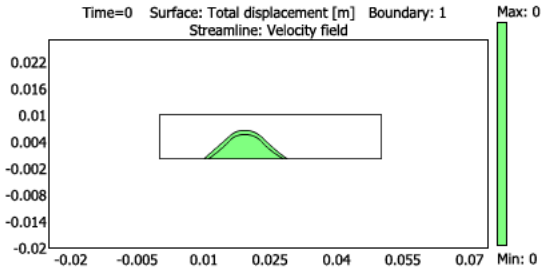

Figure 3.13: Total displacement of the plaque with a constant viscosity (μ = 0.0042) at t=0.

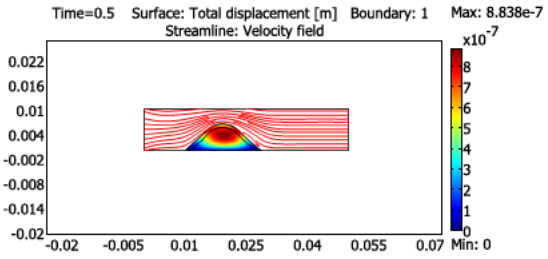

Figure 3.14: Total displacement of the plaque with a constant viscosity (μ = 0.0042) at t=0.5.

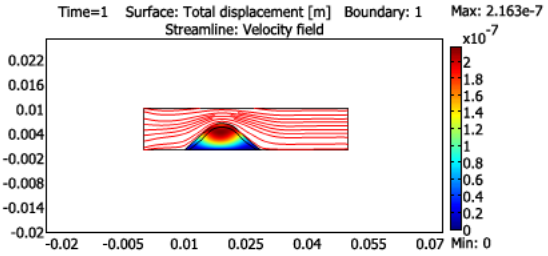

Figure 3.15: Total displacement of the plaque with a constant viscosity (μ = 0.0042) at t=1.

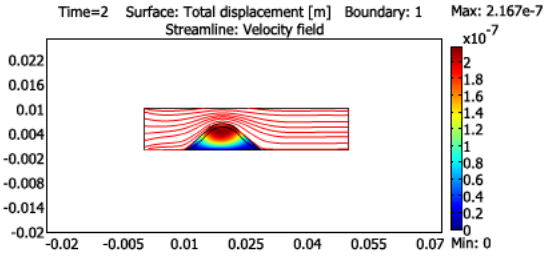

Figure 3.16: Total displacement of the plaque with a constant viscosity (μ = 0.0042) at t=2.

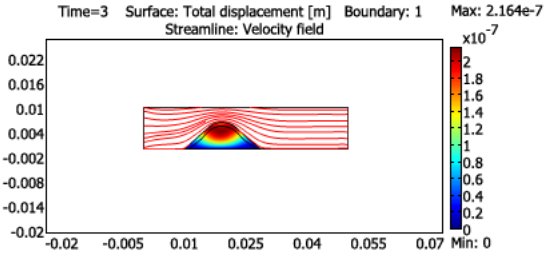

Figure 3.17: Total displacement of the plaque with a constant viscosity (μ = 0.0042) at t=3.

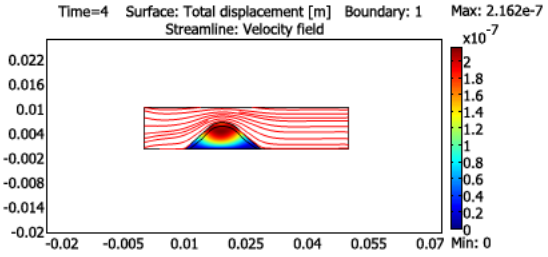

Figure 3.18: Total displacement of the plaque with a constant viscosity (μ = 0.0042) at t=4.

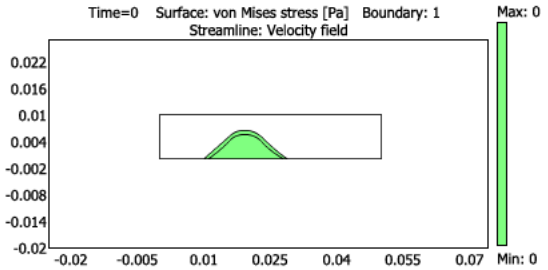

Figure 3.19: The stress over the plaque with a constant viscosity ($\mu = 0.0042$) at t=0.

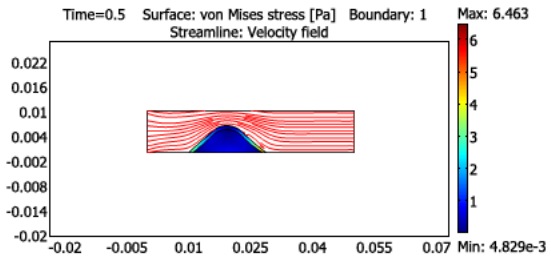

Figure 3.20: The stress over the plaque with a constant viscosity ($\mu = 0.0042$) at t=0.5.

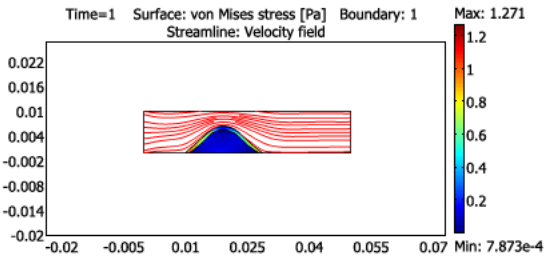

Figure 3.21: The stress over the plaque with a constant viscosity ($\mu = 0.0042$) at t=1.

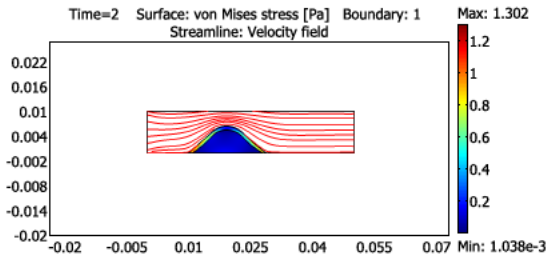

Figure 3.22: The stress over the plaque with a constant viscosity ($\mu = 0.0042$) at t=2.

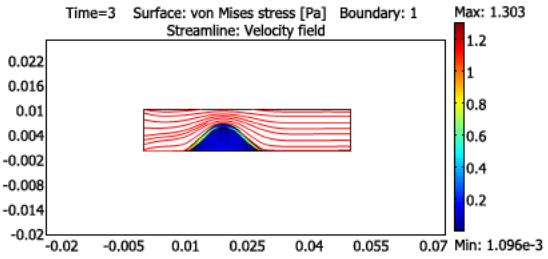

Figure 3.23: The stress over the plaque with a constant viscosity ($\mu = 0.0042$) at t=3.

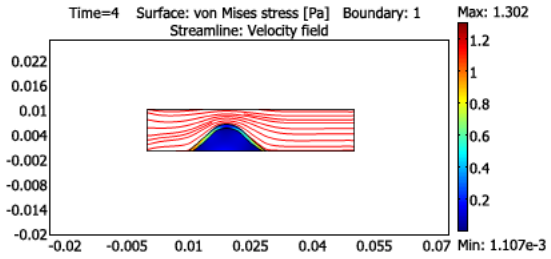

Figure 3.24: The stress over the plaque with a constant viscosity ($\mu = 0.0042$) at t=4.

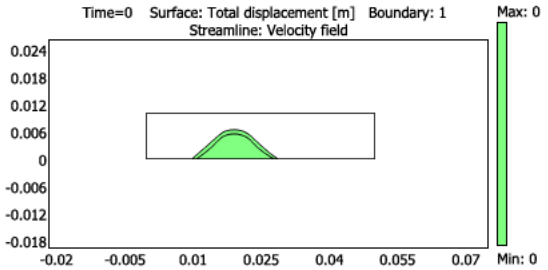

Figure 3.25: Total displacement of the plaque with a variable viscosity at t=0.

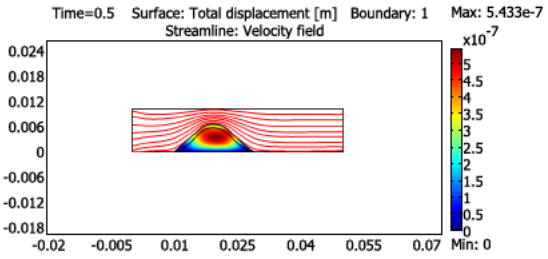

Figure 3.26: Total displacement of the plaque with a variable viscosity at t=0.5.

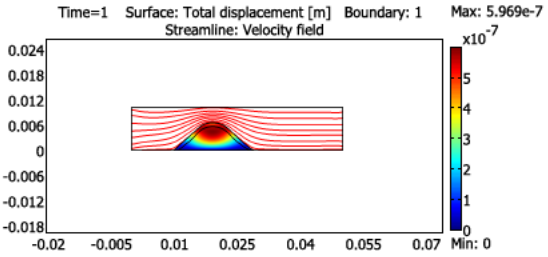

Figure 3.27: Total displacement of the plaque with a variable viscosity at t=1.

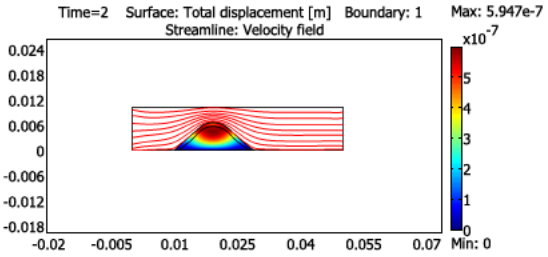

Figure 3.28: Total displacement of the plaque with a variable viscosity at t=2.

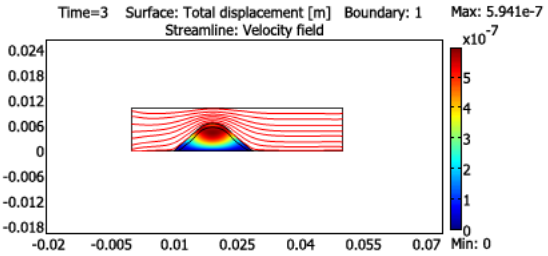

Figure 3.29: Total displacement of the plaque with a variable viscosity at t=3.

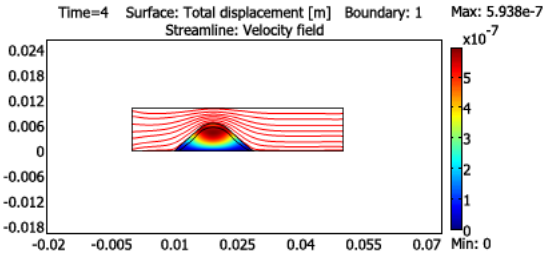

Figure 3.30: Total displacement of the plaque with a variable viscosity at t=4.

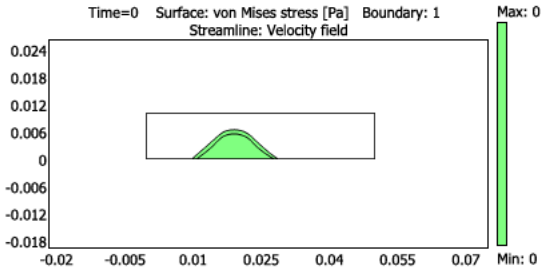

Figure 3.31: The stress over the plaque with a variable viscosity at t=0.

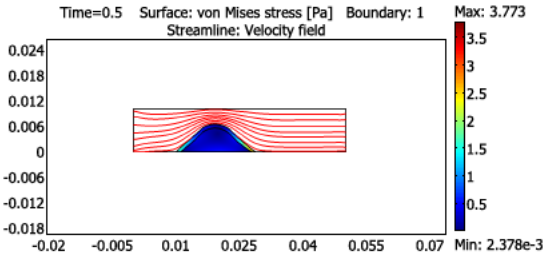

Figure 3.32: The stress over the plaque with a variable viscosity at t=0.5.

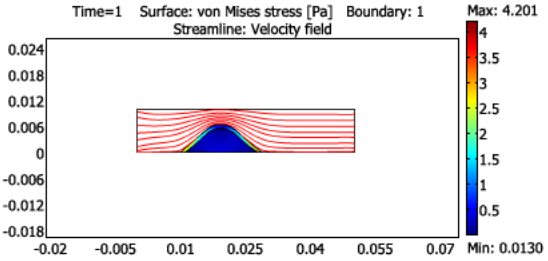

Figure 3.33: The stress over the plaque with a variable viscosity at t=1.

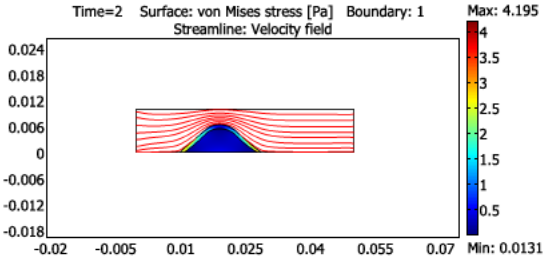

Figure 3.34: The stress over the plaque with a variable viscosity at t=2.

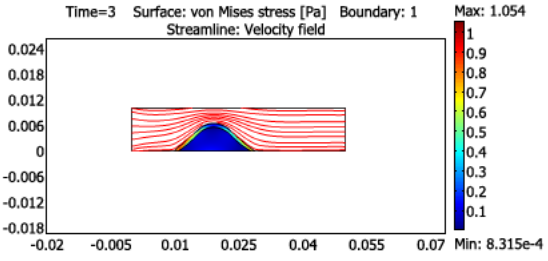

Figure 3.35: The stress over the plaque with a variable viscosity at t=3.

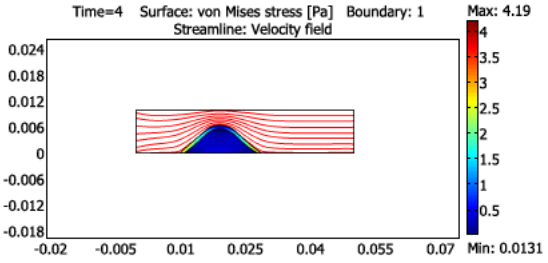

Figure 3.36: The stress over the plaque with a variable viscosity at t=4.

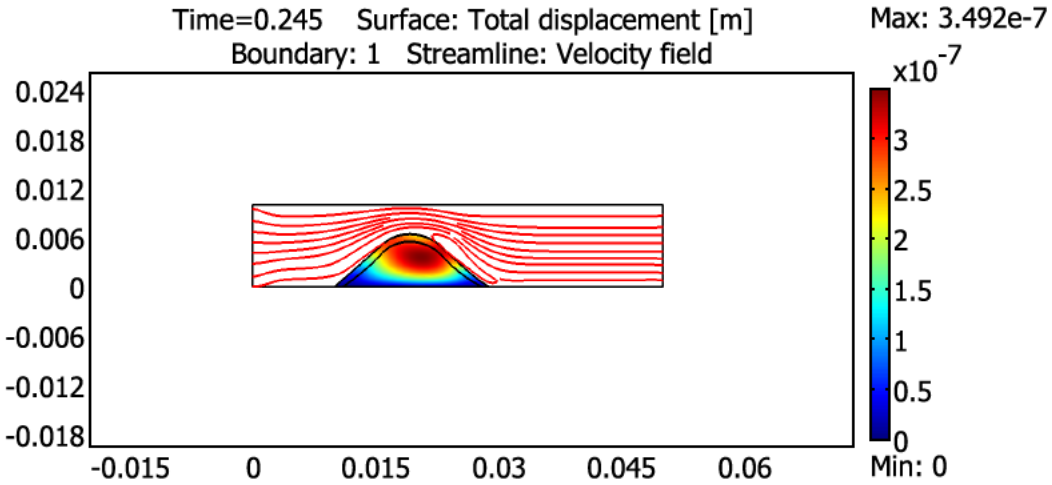

Figure 3.37: Blood recirculations for the Newtonian model.

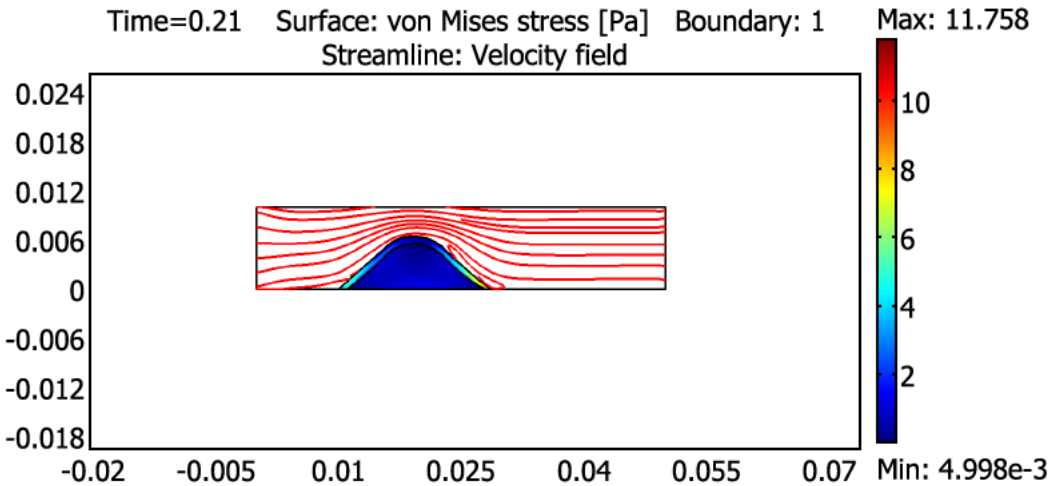

Figure 3.38: Blood recirculations for the non-Newtonian model.

Chapter 4

Discussion

In this thesis, we have developed a model for the fluid structure interaction between the blood and the plaque of atherosclerosis. The viscosity was the main key player in the presented analysis along with the velocity, density and pressure of the blood. We were able to differentiate between two different cases with respect to the viscosity: the Newtonian case and the non-Newtonian one. In addition, in the Newtonian case we have taken two different values for the viscosity which are considered low and high respectively. We have proved the existence of solution for this problem, then we tested the coupled model numerically using the ALE formulation.

The main of interests of the numerical results are the displacement of the plaque, the stress over it and the recirculations of the blood. The comparison between Fig.3.6, Fig.3.18 and Fig.3.30 showed that the displacement of the plaque is more important in the non-Newtonian case than the Newtonian one in the two cases where $\mu = 0.0035$ and for $\mu = 0.0042$. The ratio between the maximal displacement of the plaque where we have a variable viscosity and the one where we have a high viscosity is equal to 1.087 and the ratio between the model with a variable viscosity and the one where the viscosity is low is 1.113. Results obtained are expected because the viscosity in the Newtonian case (low one) is the minimal value of the apparent viscosity taken in the non-Newtonian model, and the one taken in the Newtonian model (high viscosity) is less then the maximal value of the apparent viscosity taken in the non-Newtonian one. The second main of interest is the stress over the plaque for the three cases. From Fig.3.24, Fig.3.12 and Fig.3.36 the maximal value is about 85.741 Pa for the non-

Newtonian model, 78.285 Pa for the Newtonian model(high viscosity) and 76.018 Pa for the Newtonian model(low viscosity). The ratio between the maximal Von Mises stress in the non-Newtonian model and the Newtonian one where the viscosity is high is about 1.095, and about 1.127 between the non-Newtonian model and the Newtonian one where the viscosity is low. These results are also expected and show that the model where the viscosity is high overestimates the stress over the plaque and this may lead to the rupture of the plaque and overestimate this risk as well.

The third main of interest is the recirculation of the blood that increased the possibility of clot formation in the dead zones of the blood flow. From Fig.3.37 and Fig.3.38, we can notice that recirculations of the blood is more important in the Newtonian case where the viscosity is low than the two other models. The recirculations zones are minimized in the non-Newtonian model where the viscosity is greater than the Newtonian case.

Coronavirus disease 2019 lead to many changes in the patient's body, this new virus not only affects the respiratory system but also can cause several changes in the hematological and the rheological properties of the blood. An increase in the Red Blood Cells aggregation is a result of this virus lead to an increase in the viscosity of the blood [22]. So we can say that the Newtonian model where the viscosity is high $\mu = 0.0042$ corresponds to a covid 19 patients.

The summary of the results obtained are represented in table 4.1.

Flow Parameters	**Normal case**	**Hyper viscous case**	**non-Newtonian**
Von Mises stress	76.018 Pa	78.285 Pa	85.741 Pa
Total displacement	$1.109e^{-5}$	$1.136e^{-5}$	$1.235e^{-5}$
Number of recirculation	2	2	1

Table 4.1: Comparison of the results obtained for the both models (non-Newtonian and Newtonian (normal and covid)).

This research can be expanded by considering different degrees of stenosis and studying the blood flow and the stress distribution for every case. In addition, we can vary the boundary conditions of the wall (rigid, compliant) and extend our work to a 3D case.

Bibliography

[1] Telma Silva, Adélia Sequeira, Rafael F Santos, and Jorge Tiago. Mathematical modeling of atherosclerotic plaque formation coupled with a non-newtonian model of blood flow. 2013, 2013.

[2] https://www.melbourneheartcare.com.au/for-patients/conditions/atherosclerosis/.

[3] Number of deaths by cause, world, 2017. `https://ourworldindata.org/grapher/annual-number-of-deaths-by-cause?country=~OWID_WRL`.

[4] Hiba Deek, Phillip Newton, Sally Inglis, Samer Kabbani, Samar Noureddine, Peter S. Macdonald, and Patricia M. Davidson. Heart health in lebanon and considerations for addressing the burden of cardiovascular disease. *Collegian*, 22(3):333–339, 2015.

[5] H Harb. Statistical bulletin, 2011.

[6] Alistair Farley, Charles Hendry, and Ella McLafferty. Blood components. *Nursing Standard (through 2013)*, 27(13):35, 2012.

[7] Bruce Roy Munson, Theodore Hisao Okiishi, Wade W Huebsch, and Alric P Rothmayer. *Fluid mechanics*. Wiley Singapore, 2013.

[8] John A Dormandy. Influence of blood viscosity on blood flow and the effect of low molecular weight dextran. *Br Med J*, 4(5789):716–719, 1971.

[9] Rajendra P Chhabra. Non-newtonian fluids: an introduction. In *Rheology of complex fluids*, pages 3–34. Springer, 2010.

[10] Sunanda Saha, Anuradha Bhattacharjee, et al. A 2d fsi mathematical model of blood flow to analyze the hyper-viscous effects in atherosclerotic covid patients. *Results in Engineering*, 12:100275, 2021.

[11] Nader El Khatib, Stéphane Génieys, AM Zine, and Vitaly Volpert. Non-newtonian effects in a fluid-structure interaction model for atherosclerosis. *Journal of technical physics*, 50(1):55–64, 2009.

[12] S Boujena, Oualid Kafi, and N El Khatib. A 2d mathematical model of blood flow and its interactions in an atherosclerotic artery. *Mathematical Modelling of Natural Phenomena*, 9(6):46–68, 2014.

[13] Maryse Bourlard-Jospin and Serge Nicaise. Abstract green formula and applications to integral equations. *Numerical Functional Analysis and Optimization*, 18:667–689, 01 1997.

[14] HENDRA Gunawan. On n-inner products, n-norms, and the cauchy-schwarz inequality. *Scientiae Mathematicae Japonicae*, 55(1):53–60, 2002.

[15] A Quarteroni and L Formaggia. Computational models for the human body. *Handbook of Numerical Analysis*, 12:7–15, 2004.

[16] John M Holte. Discrete gronwall lemma and applications. 24:1–7, 2009.

[17] Sunanda Saha, Anuradha Bhattacharjee, et al. A 2d fsi mathematical model of blood flow to analyze the hyper-viscous effects in atherosclerotic covid patients. *Results in Engineering*, 12:100275, 2021.

[18] RE Holsworth and JV Wright. Blood viscosity: the unifying parameter in cardiovascular disease risk. *Holistic Primary Care*, 13:1–2, 2012.

[19] Beuy Joob and Viroj Wiwanitkit. Blood viscosity of covid-19 patient: a preliminary report. *American journal of blood research*, 11(1):93, 2021.

[20] Oualid Kafi, Nader El Khatib, Jorge Tiago, and Adélia Sequeira. Numerical simulations of a 3d fluid-structure interaction model for blood flow in an atherosclerotic artery. *Mathematical Biosciences & Engineering*, 14(1):179, 2017.

[21] Shewaferaw S Shibeshi and William E Collins. The rheology of blood flow in a branched arterial system. *Applied Rheology*, 15(6):398–405, 2005.

[22] Beuy Joob and Viroj Wiwanitkit. Blood viscosity of covid-19 patient: a preliminary report. *American journal of blood research*, 11(1):93, 2021.